Article

Cell Chemical Biology

Talaromyces marneffei Mp1p Is a Virulence Factor that Binds and Sequesters a Key Proinflammatory Lipid to Dampen Host Innate Immune Response

Highlights

- *T. marneffei* Mp1p uses LBD2 to capture proinflammatory lipid mediator arachidonic acid
- Mp1p-LBD2 forms a five-helix bundle fold to bind one or two arachidonic acids
- Mp1p-LBD2 homologs are also found in other pathogenic fungi
- A novel virulence mechanism to evade host immunity was discovered

Authors

Kong-Hung Sze, Wai-Hei Lam, Hongmin Zhang, ..., Richard Y.T. Kao, Quan Hao, Kwok-Yung Yuen

Correspondence

rytkao@hku.hk (R.Y.T.K.), qhao@hku.hk (Q.H.), kyyuen@hku.hk (K.-Y.Y.)

In Brief

Sze et al. find that a *Talaromyces marneffei* protein, Mp1p, traps a key proinflammatory lipid mediator arachidonic acid with high affinity. This represents an interesting, previously unknown virulence mechanism of evading the host innate immune defense by pathogenic fungi.

Accession Numbers

5CSD
5FB7

Sze et al., 2017, Cell Chemical Biology *24*, 182–194
February 16, 2017
http://dx.doi.org/10.1016/j.chembiol.2016.12.014

Please cite this article as: Sze et al., *Talaromyces marneffei* Mp1p Is a Virulence Factor that Binds and Sequesters a Key Proinflammatory Lipid to Dampen Host Innate Immune Response, Cell Chemical Biology (2017), http://dx.doi.org/10.1016/j.chembiol.2016.12.014

Talaromyces marneffei Mp1p Is a Virulence Factor that Binds and Sequesters a Key Proinflammatory Lipid to Dampen Host Innate Immune Response

Kong-Hung Sze,[1,2,3,4,8] Wai-Hei Lam,[5,6,8] Hongmin Zhang,[5,6,7,8] Yi-hong Ke,[1,2,3,4,8] Man-Kit Tse,[1,2,3,4,8] Patrick C.Y. Woo,[1,2,3,4] Susanna K.P. Lau,[1,2,3,4] Candy C.Y. Lau,[1,2,3,4] Jian-piao Cai,[1,2,3,4] Edward T.K. Tung,[1] Raymond K.C. Lo,[1,2,3,4] Simin Xu,[1,2,3,4] Richard Y.T. Kao,[1,2,3,4,*] Quan Hao,[5,6,*] and Kwok-Yung Yuen[1,2,3,4,9,*]

[1]State Key Laboratory of Emerging Infectious Diseases
[2]Department of Microbiology
[3]Research Centre of Infection and Immunology
[4]Carol Yu Centre for Infection
[5]School of Biomedical Sciences
The University of Hong Kong, Hong Kong SAR, China
[6]Shenzhen Institute of Research and Innovation, The University of Hong Kong, Shenzhen 518000, China
[7]Department of Biology, Shenzhen Key Laboratory of Cell Microenvironment, Southern University of Science and Technology, Shenzhen 518055, China
[8]Co-first author
[9]Lead Contact
*Correspondence: rytkao@hku.hk (R.Y.T.K.), qhao@hku.hk (Q.H.), kyyuen@hku.hk (K.-Y.Y.)
http://dx.doi.org/10.1016/j.chembiol.2016.12.014

SUMMARY

Talaromyces (Penicillium) marneffei **is one of the leading causes of systemic mycosis in immunosuppressed or AIDS patients in Southeast Asia. How this intracellular pathogen evades the host immune defense remains unclear. We provide evidence that *T. marneffei* depletes levels of a key proinflammatory lipid mediator arachidonic acid (AA) to evade the host innate immune defense. Mechanistically, an abundant secretory mannoprotein Mp1p, shown previously to be a virulence factor, does so by binding AA with high affinity via a long hydrophobic central cavity found in the LBD2 domain. This sequesters a critical proinflammatory signaling lipid, and we see evidence that AA, AA's downstream metabolites, and the cytokines interleukin-6 and tumor necrosis factor α are downregulated in *T. marneffei*-infected J774 macrophages. Given that Mp1p-LBD2 homologs are identified in other fungal pathogens, we expect that this novel class of fatty-acid-binding proteins sequestering key proinflammatory lipid mediators represents a general virulence mechanism of pathogenic fungi.**

INTRODUCTION

Talaromyces marneffei (previously known as *Penicillium marneffei*) has emerged as a significant pathogen, which causes potentially fatal systemic mycosis in immunocompromised patients in Southeast Asia and China (Cooper and Vanittanakom, 2008; Ustianowski et al., 2008; Vanittanakom et al., 2006; Wong et al., 1999). Infection by *T. marneffei* is now recognized as an AIDS-indicator disease. The disease may not appear in some infected persons until they develop immune dysfunction years after exposure to this fungus. This latency in disease development suggests that *T. marneffei* can evade clearance by a normally functioning immune system. Despite its medical importance, little is known about the molecular mechanisms underlying its pathogenesis and how it evades the host defense to survive in the harsh intracellular environment of macrophages (d'Enfert, 2009; Vanittanakom et al., 2006).

Mp1p was the first characterized secretory protein of *T. marneffei* (Cao et al., 1998). Mp1p encodes a protein of 462 amino acid residues with three domains: ligand binding domain 1 (LBD1, residues 22–180), ligand binding domain 2 (LBD2, residues 187–346), and a serine and threonine-rich domain near the C terminus. Mp1p is present in the yeast phase of the fungus and abundantly found in the sera of patients suffering from penicilliosis marneffei (Cao et al., 1999). Therefore, Mp1p was used for serodiagnosis for *T. marneffei* infections (Cao et al., 1998). We have recently shown unambiguously that Mp1p is a novel virulence factor of *T. marneffei* by performing knockout and knockdown experiments using an intracellular survival assay with murine macrophage cells and mouse challenge models (Woo et al., 2016). In particular, all mice died within 21 days after intravenous challenge with the wild-type *T. marneffei* strain, whereas none of the mice died even 60 days after challenge with the Mp1p gene (*MP1*) knockout strain. However, the mechanism of virulence of Mp1p remains unclear. Despite our previous characterization of Mp1p showing that the recombinant Mp1p-LBD2 has a fatty-acid-binding domain and forms a helix bundle dimeric complex in 1:1 molar ratio with palmitic acid (PLM) copurified from an *Escherichia coli* expression system (Liao et al., 2010), the actual cellular target substrate of Mp1p-LBD2 is still unknown.

Here, we applied pull-down experiments to discover that the key proinflammatory mediator, arachidonic acid (AA), was the

dominant high-affinity cellular target of Mp1p-LBD2. Subsequently, we solved the crystal structures of Mp1p-LBD2 in complex with AA. Mp1p-LBD2 formed a five-helix bundle monomeric structure with a long hydrophobic central cavity for high-affinity encapsulation of cellular AA. Furthermore, Mp1p-LBD2 has an unusual plasticity of trapping one or two molecules of AA depending on the availability of AA. This strong and flexible binding of Mp1p-LBD2 with AA was also validated by nuclear magnetic resonance (NMR) titration and isothermal titration calorimetry (ITC) experiments.

The first-line defense of our body against microbial infection is achieved through the activation of proinflammatory mediators to signal and attract immune components to the site of infection (Dennis and Norris, 2015). Many of these proinflammatory mediators are lipid molecules derived from AA. AA is a key proinflammatory mediator because it is produced as a main eicosanoid precursor in response to microbial infection, which can generate many downstream prostaglandins and thromboxanes by cyclooxygenase (COX), leukotrienes and lipoxins by lipoxygenases (LOXs), and epoxyeicosatrienic acids by cytochrome P450 (CYP450) enzymes. AA-derived eicosanoids belong to a complex family of lipid mediators that regulate a wide variety of physiological processes including immune response. The eicosanoids and their receptors cooperate with other signaling molecules, particularly cytokines and chemokines, and play a crucial role in modulating physiological processes in both homeostatic and inflammatory conditions. Eicosanoid production is considerably increased during inflammation, and their biosynthetic pathways are involved in the pathogenesis of infectious diseases. We hypothesized that the high abundance of Mp1p in the sera of patients suffering from penicilliosis marneffei (Cao et al., 1999) and its ability to trap lipid molecules may enable Mp1p to function as a scavenger of the proinflammatory AA signaling mediator to suppress the host inflammatory response.

Subsequently, we have performed cell-based experiments to investigate the biological significance of capturing AA by Mp1p. Our comparative quantitative liquid chromatography-mass spectrometry (LC-MS) analysis showed that J774 cells infected with wild-type *T. marneffei* have a lower concentration of AA and lower downstream AA metabolites and cytokine interleukin-6 (IL-6) and tumor necrosis factor α (TNF-α) production in contrast to those observed in J774 cells infected with the *MP1* knockout strain. Taken together, these results reveal that Mp1p is an important virulence factor for the intracellular survival of *T. marneffei* through a novel virulence mechanism of trapping proinflammatory AA to evade the host innate immune defense.

RESULTS

AA Is a Dominant Cellular Target of Mp1p-LBD2

To identify a potential cellular target of Mp1p-LBD2, we have performed in vitro pull-down experiments on the cell lysate of J774 macrophage cells using recombinant His-tagged Mp1p-LBD2 protein. Lipopolysaccharide (LPS) is the standard chemical for inducing the inflammatory responses with upregulation of cytokines, the lipid mediators, and their metabolites. Therefore, we used LPS-activated J774 cells in our pull-down experiment to better simulate the lipid profile in infected macrophages. We have also performed Mp1p quantification by ELISA as described in the Supplemental Experimental Procedures, and the cellular level of Mp1p at 48 hr post-infection was estimated to be 0.864 ± 0.061 pmol per 1 × 10^6 J774 cells infected by the wild-type strain of *T. marneffei* (Table S1). The cellular levels of potential lipid substrates of Mp1p-LBD2 were measured by LC-MS quantification (Supplemental Experimental Procedures) for normal non-infected and LPS-activated J774 cells and are summarized in Table S2. Since the physiological cellular concentration of Mp1p is lower than the feasible operational limit of the in vitro pull-down experiment, we have performed the experiment using a bait protein in a matching range of physiological concentrations of cellular lipids. Furthermore, progressively lower amounts of Mp1p-LBD2 were used in a series of pull-down experiments in order to reveal which cellular substrates of Mp1p-LBD2 may be the dominant substrates under the condition of limited amount of Mp1p-LBD2. Figure 1A summarizes the list of identified substrates obtained from the pull-down experiment against the cell lysate of 3 × 10^6 LPS-activated J774 cells. Figure 1A shows the amount of each lipid pulled down by Mp1p-LBD2 in nanomoles and in pull-down efficiency as measured by the percentage of different lipids in cell (the amount being pulled down relative to the corresponding amount as cellular lipid as reported in Table S2). When 1,000 μg of bait protein Mp1p-LBD2 (23.0-fold AA_o, where AA_o is the equivalent amount of AA in the 3 × 10^6 LPS-activated J774 cells) was used, AA, five lysophosphatidylcholines (LPCs), PLM, and oleic acid were found in the pull-down profile list with percentages in cell pull-down efficiencies ranging from 36.2% to 98.2%. At 250 μg of Mp1p-LBD2 (5.7-fold AA_o), the same list of lipids was found in the pull-down extract but all lipids were significantly decreased in amount and pull-down percentage except for AA. At the lowest amount of bait protein of 50 μg of Mp1p-LBD2 (1.1-fold AA_o), all LPCs were no longer detectable in the pull-down list. Again, only AA maintained its cellular pull-down amount of about 1.7 nmol and became the dominant substrate while PLM and oleic acid were reduced further to 0.3 and 0.1 nmol, respectively. These results indicated that Mp1p-LBD2 is capable of binding to a number of cellular lipid substrates but, at the lower limit of Mp1p-LBD2 concentration, AA will dominate over other cellular lipid substrates even though AA was the lowest amount in the list of cellular lipids (Table S2). This implies that AA is the dominant cellular target of Mp1p-LBD2 with higher affinity of binding to Mp1p-LBD2. The chemical identities of AA, PLM, and oleic acid in the pull-down lipid extracts were confirmed by using pure standards (Supplemental Experimental Procedures). The identities of the observed LPCs were classified to these lipid classes by their tandem mass spectrometry (MS/MS) fragmentation patterns (Figure 1C, Supplemental Experimental Procedures and Table S3).

Mp1p-LBD2's Binding with AA Showed a Two-Step Binding Curve

The specific binding of AA with Mp1p-LBD2 was validated by titration of AA into an ^{15}N-labeled sample of Mp1p-LBD2. Figure 2A shows the overlaid two-dimensional (2D) ^{1}H-^{15}N heteronuclear single quantum coherence (HSQC) NMR spectra of delipidated ^{15}N-labeled Mp1p-LBD2 (red-colored cross peaks) and delipidated ^{15}N-labeled Mp1p-LBD2 after the addition of

A

Lipid in pull-down extract, (m/z)	50 μg (1.1 AA_o)		250 μg (5.7 AA_o)		1000 μg (23.0 AA_o)	
	nmol[a]	% in cell[b]	nmol[a]	% in cell[b]	nmol[a]	% in cell[b]
AA, 303.2323	1.72	81.9%	1.7	81.0%	1.78	84.8%
Palmitic acid, 255.2	0.3	3.1%	1.2	12.5%	8.8	91.7%
Oleic Acid, 283.3	0.1	1.2%	0.6	7.1%	3.6	42.9%
LPC1, 482.3617	-	-	1.4	24.6%	5.6	98.2%
LPC2, 522.3555	-	-	1.8	23.1%	7.5	96.2%
LPC3, 496.34	-	-	2.8	17.9%	12.8	81.9%
LPC4, 524.3727	-	-	0.5	13.9%	3.4	94.4%
LPC5, 544.3365	-	-	0.7	10.1%	2.5	36.2%

a Values collected from $3x10^6$ LPS-activated cells used for pull-down
b Pull-down efficiency measured as percentage in cell relative to its corresponding cellular lipid amount reported in Supplemental Table S2

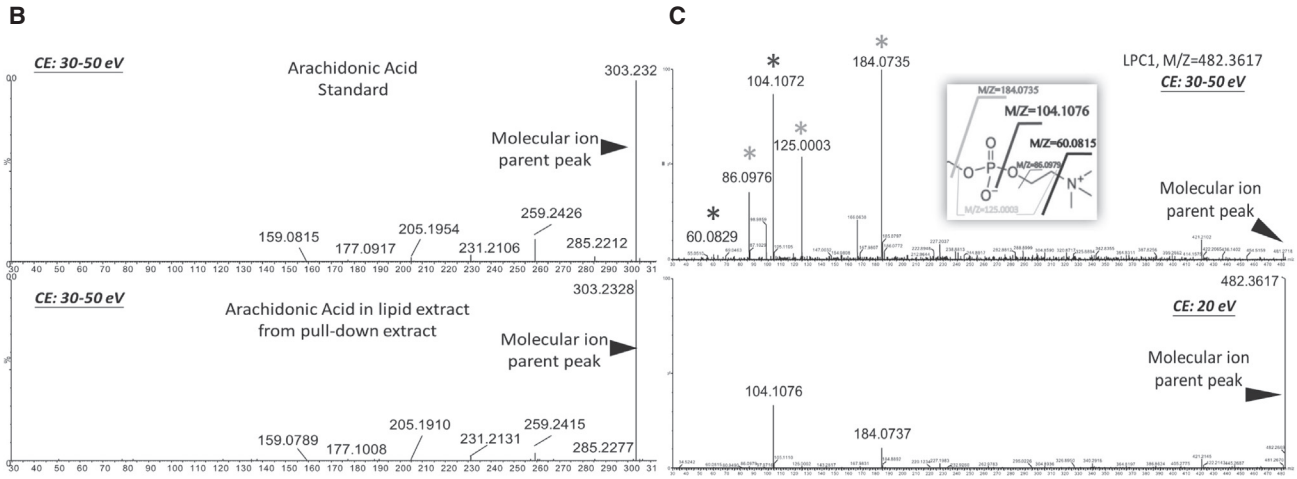

Figure 1. In Vitro Pull-Down Experiments with Various Amounts of Mp1p-LBD2 against Cell Lysates of J774 Macrophage Cells

(A–C) Profile list of identified lipids from the organic layer extracted under different amounts of Mp1p-LBD2 bait protein (A). MS/MS spectra of the precursor ions $[M - H]^-$ at m/z 303.2328 (B) and 184.0735 (C) corresponding to arachidonic acid and lysophosphatidylcholine (LPC) head group (inset), respectively. The identity of each LPC in (A) was not characterized. All LPC ions give rise to the same characteristic fragment ion (m/z 184.0735) in high-energy mode (collision energy [CE] = 30–50 eV). The general structure and the predicted fragmentation positions are given in the inset of (C).

2.5 molar equivalent of AA (blue-colored cross peaks). The three expansion insets of ^1H-^{15}N HSQC spectra in Figure 2B show the movements of cross peaks at the AA to Mp1p-LBD2 molar ratios of 0, 0.5, 1.25, 1.75, and 2.5 using different cross-peak color coding. Many amide cross peaks of Mp1p-LBD2 showed large and specific changes upon the addition of AA, indicating that the binding was site specific. Figure 2C shows the titration curves of representative residues Asp238, Gly239, Leu255, Val258, Glu280, and Leu282. It should be noted that these titration curves displayed two-step curves, which were consistent with the observations of change of chemical shift perturbation directions in many cross peaks. One of them is demonstrated in the inset box of residue Asp238 in Figure 2B. These results indicated that Mp1p-LBD2 could bind to more than one AA molecule. The first titration step started at [AA]:[Mp1p-LBD2] = 0:1 and ended at ratio 1:1, which are indicative of a higher affinity binding site (Figure 2C). The second step started at a ratio around 1–1.25:1 and leveled off at a ratio of ~2.5:1, representing a weaker affinity binding site (Figure 2C). Figure 3A shows the ITC raw heats of binding and isotherms of AA titrated into wild-type Mp1p-LBD2 and its I332A and V309D mutants. The isotherm for titration of AA into wild-type Mp1p-LBD2 also showed a two-step curve and was best fitted with a two-state model. Fitting of the ITC isotherm with a two-state model gave the first binding site a high-affinity K_d of 13 nM, while the second binding site had a moderate-affinity K_d of 2.3 μM. But the isotherms of the two Mp1p-LBD2 mutants (I332A and V309D) were best fitted with a single-state model (Figures 3A and 3B). These mutants were constructed to evaluate the effects of mutating a key interacting residue near the center of each binding site. Figure 3B shows that these mutants have significantly weakened the binding of AA with Mp1p-LBD2 (K_d = 1700 and 3,800 nM for I332A and V309D mutants, respectively) and reduced the isotherms to single-step curves. Consistent with the ITC findings, the NMR chemical shift perturbation titration curves of these mutants demonstrated on residue Asp263 were also switched to one-step curves (Figure 2D).

Crystal Structure of Mp1p-LBD2 Binding with One AA Molecule

Mp1p-LBD2 was crystallized with an equal molar ratio of AA in space group C2 with four Mp1p-LBD2s in the crystallographic asymmetric unit (Table S6 and Figure S1A). There were minimal contacts between Mp1p-LBD2 and its symmetry-related

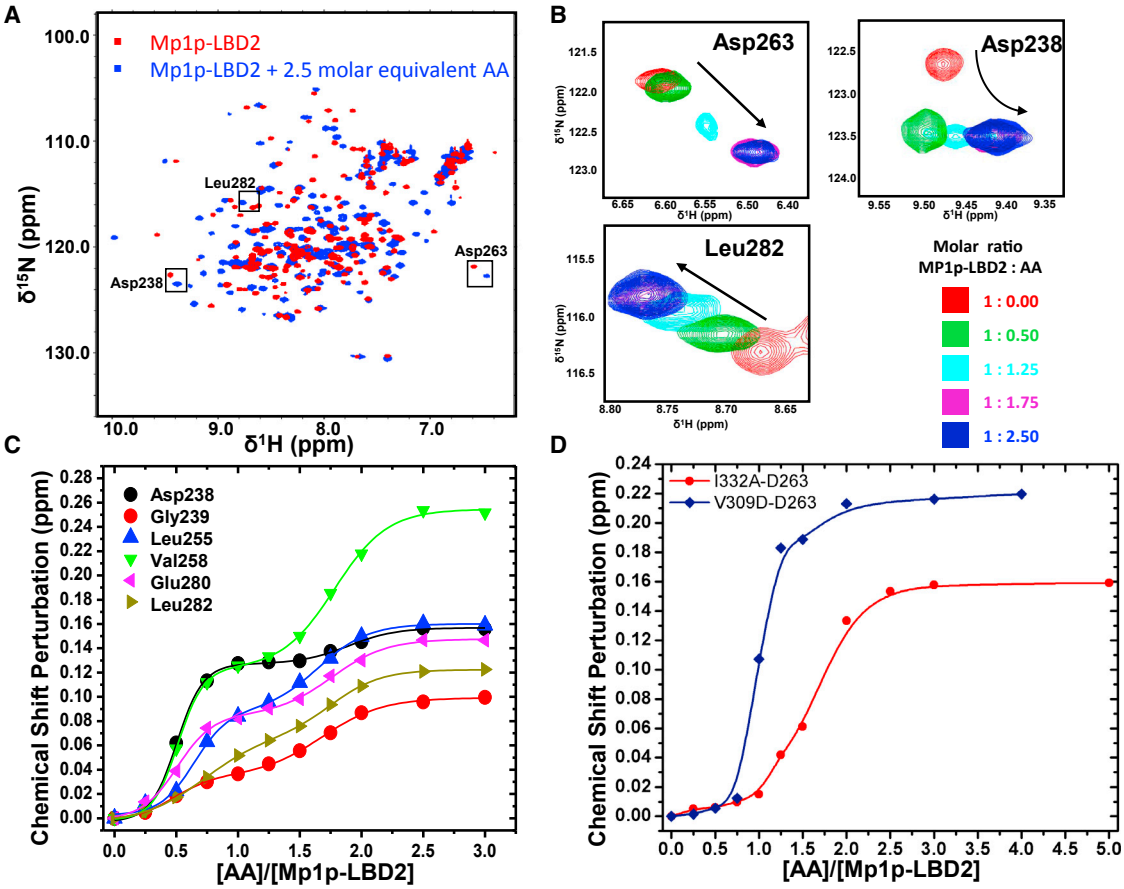

Figure 2. NMR Titration Experiments of ^{15}N-Labeled Mp1p-LBD2 with AA

(A) ^{1}H-^{15}N HSQC titration spectra of ^{15}N-labeled Mp1p-LBD2 in the absence (red) and presence (blue) of 2.5 molar equivalent of AA.

(B) Expanded views of selected residues in the absence of AA (red) and with increasing (green to blue) molar equivalent ratios of AA.

(C) Chemical shift perturbation curves of representative residues (Asp238, Gly239, Leu255, Val258, Glu280, and Leu282) versus [AA]/[Mp1p-LBD2].

(D) Chemical shift perturbation curves of residue Asp263 versus AA for Mp1p-LBD2 mutants I332A and V309D showing a switch to one-step titration curve.

molecules. This indicated that Mp1p-LBD2 was a monomer, which was consistent with the gel filtration assay results (Supplemental Experimental Procedures and Figure S2). The structure of Mp1p-LBD2 was composed of five long helices packed as a bundle (Figure 4A). Previously, we showed that Mp1p-LBD2 formed a dimer with two PLM molecules in the central cavities of two five-helix bundles. Each of the bundles was composed of two helices from one monomer and the remaining three helices from the other monomer (PDB: 3L1N) (Liao et al., 2010). In contrast to the dimeric Mp1p-LBD2-PLM structure, Mp1p-LBD2 bound with one AA (Mp1p-LBD2-1AA) was a monomer. The AA molecule was located in the central binding cavity of the Mp1p-LBD2 monomer. Most of the amino acid residues in the central binding cavity were hydrophobic and none of them were charged. Residues of Mp1p-LBD2 involved in the hydrophobic interaction network with AA were Phe196, Val199, Ile200, Thr236, Leu249, Ala254, Leu257, Val261, Leu264, Ile268, Val309, and Ile328. In addition, the AA also formed hydrogen bonds with residue Gln298 of Mp1p-LBD2. But this interaction was not observed in the Mp1p-LBD2-PLM structure (Liao et al., 2010).

Alignment between the Mp1p-LBD2-PLM structure exhibiting a domain-swapped dimeric conformation (PDB: 3L1N) and the monomeric Mp1p-LBD2-1AA structure is shown in Figure S3A (magenta, Mp1p-LBD2-1AA; green, N-terminal half of the helical barrel in 3L1N; blue, the remaining half of the helical barrel from adjacent Mp1p-LBD2-PLM in crystal packing, in 3L1N). Singly bound AA (magenta) and PLM (green) were positioned differently in the hydrophobic cavity of Mp1p-LBD2. Their carboxyl ends pointed to opposite directions in the helical barrel. Most parts of the protein from the two structures aligned well, except at the N-terminal ends of the third helices around Gly259 (regions enclosed by an orange box), where a bend was observed in Mp1p-LBD2-PLM but not in Mp1p-LBD2-1AA nor Mp1p-LBD2-2AA (not shown here for clarity). Figure S3B shows a close-up view of the additional hydrophobic interactions between the carbon chain of AA in the monomeric Mp1p-LBD2-1AA structure and the amino acid residues at the region flanking Gly259. Only side chains are shown for clarity; the two Gly259 residues in the dimer are shown in full, with the same color coding as in Figure S3A. As a result, this part of the third helix was positioned closer to the bound AA and continued in the

A

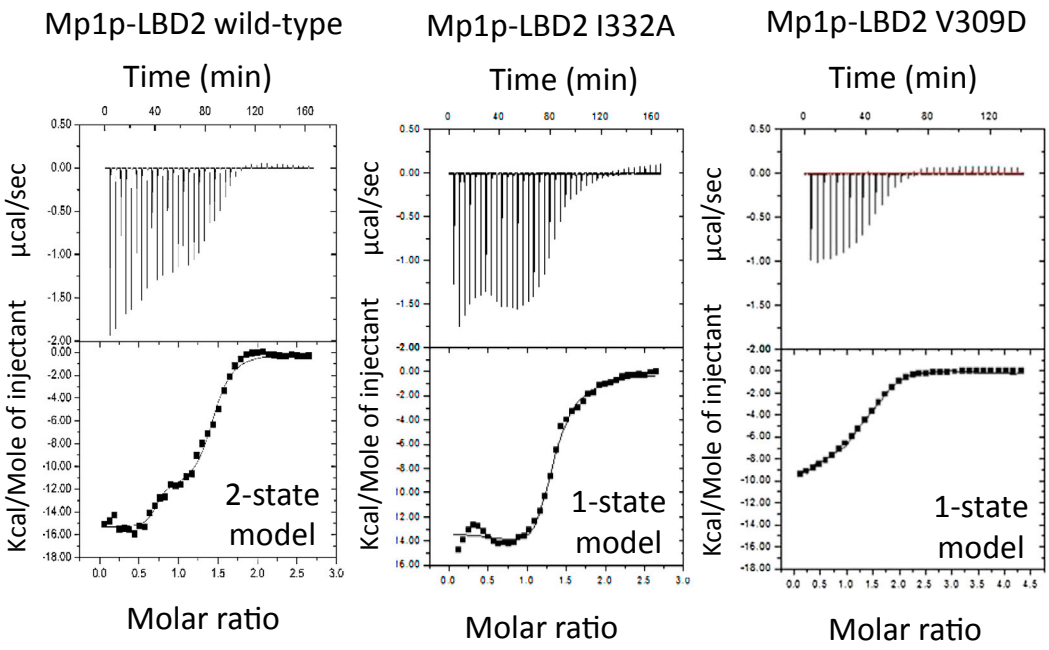

B

Analyte	N_1	Kd_1 X 10^{-9} (M)	ΔH_1 (Kcal/mol)	$-T\Delta S_1$ (Kcal/mol)	N_2	Kd_2 X 10^{-6} (M)	ΔH_2 (Kcal/mol)	$-T\Delta S_2$ (Kcal/mol)
Mp1p-LBD2 wild-type	0.67	13	-14.2	3.4	0.81	2.3	-11.0	2.3
Mp1p-LBD2 I332A	1.25	1700	-14.5	6.4	-	-	-	-
Mp1p-LBD2 V309D	1.32	3800	-9.3	1.9	-	-	-	-

Figure 3. Isothermal Titration Calorimetry of AA Binding to Mp1p-LBD2

(A) (Top row) Raw heats of binding obtained by ITC when AA was mixed with the wild-type Mp1p-LBD2 and its I332A and V309D mutants, respectively. (Bottom row) Binding isotherms fitted to the raw data using two-state or single-state binding models as indicated.

(B) Table of thermodynamic parameters obtained by fitting the ITC data to a two-state or single-state binding model (K_d, dissociation constant; ΔH, change in enthalpy; $-T\Delta S$, change in entropy; N, number of binding sites, subscripts 1 and 2 refer to the first and second binding step for data fit to a two-state model).

same direction. Thus, no sharp bending was observed. However, these hydrophobic interactions were absent in Mp1p-LBD2-PLM due to opposite orientation of bound PLM and hence might cause this complex structure to adopt a domain-swapped state. Competition NMR titration experiment showed that PLM can be readily displaced by a lower concentration of AA, indicating that Mp1p-LBD2 has a significantly lower affinity toward PLM than AA (Supplemental Experimental Procedures and Figure S4).

Central Cavity of Mp1p-LBD2 Can Simultaneously Accommodate Two AA Molecules

We have shown that Mp1p-LBD2 can bind two molecules of AA by NMR spectroscopy and ITC measurements. To validate these results, we crystallized Mp1p-LBD2 with an excess amount of AA. Diamond-like crystals were obtained in space group C2, and there were four Mp1p-LBD2 molecules in an asymmetric unit (Table S6). Electron densities clearly showed this unusual simultaneous binding of two AA molecules in the central cavity of each Mp1p-LBD2 molecule (Figure 4B, right, and Figure S1B). The overall folding of Mp1p-LBD2 complexed with two AA molecules (Mp1p-LBD2-2AA) was identical to that of Mp1p-LBD2-1AA with a root-mean-square deviation value of 0.203 Å for all C_α atoms, indicating that the conformation of the five-helix bundle of Mp1p-LBD2 is independent of the number of bound AA molecules. The two AA molecules adopted different conformations, one was U shaped (AA_1) and the other was in extended form (AA_2). These two ligands adopted a head-to-head configuration with their carboxylic head groups pointing toward each other. Figure 4B shows that the binding of AA molecules in the central cavity of Mp1p-LBD2 was mainly through hydrophobic interactions with a large number of hydrophobic residues, such

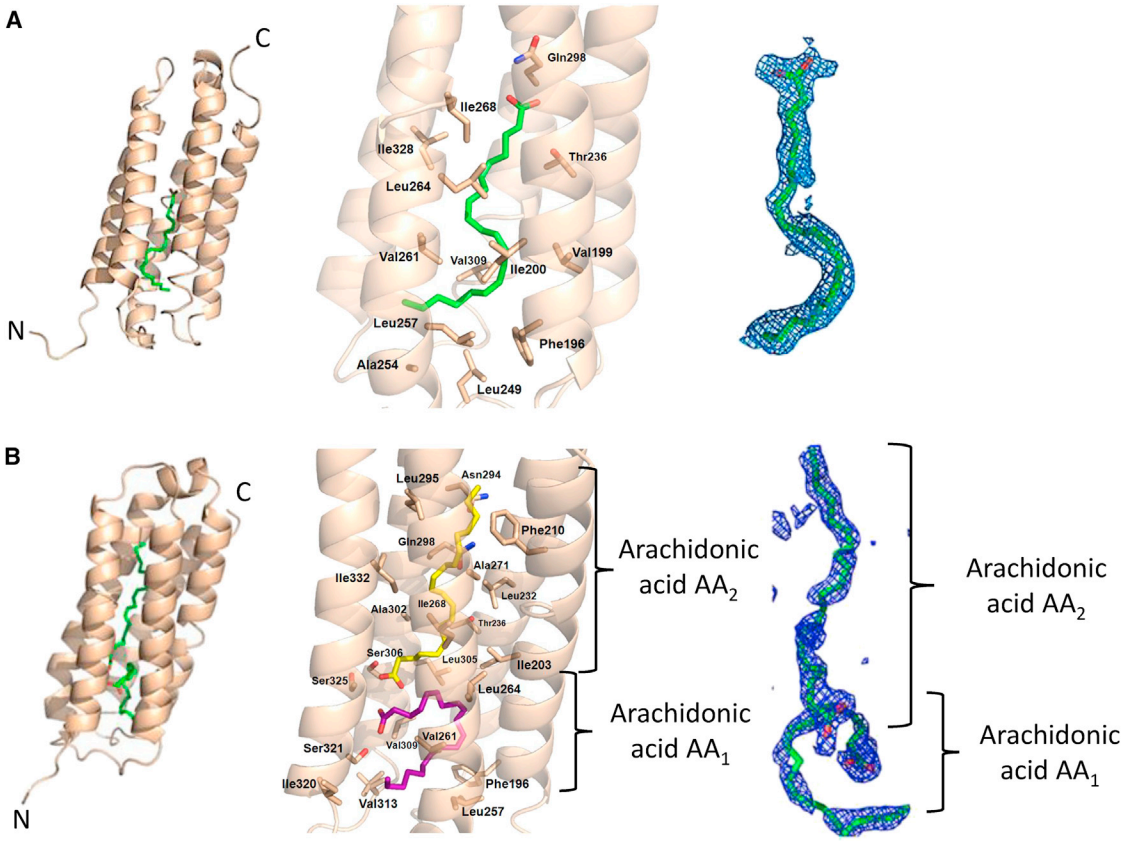

Figure 4. Crystal Structures of Mp1p-LBD2 in Complex with AA

(A and B) One AA molecule (A) and two AA molecules (B). (Left) Ribbon representation of the overall structure of the Mp1p-LBD2 complexed with AA. AA is shown as a stick in green. (Middle) Close-up view of residues in Mp1p-LBD2 involved in hydrophobic interaction with AA molecules. The interactions between the singly bound AA were mainly hydrophobic, and residue Gln298 forms an additional hydrogen bond to the carboxylic head group of AA. The interactions between the doubly bound AAs (AA_1, purple, and AA_2, yellow) and Mp1p-LBD2 were mainly hydrophobic. Residues Ser306, Ser321, and Ser325 provided additional hydrogen bonds to the carboxylic head groups of the bound AAs. (Right) $F_o - F_c$ omit maps of the singly bound (contour level of 3.0σ) and doubly bound (contour level of 2.8σ) AAs showing clear densities of both AA molecules.

as Phe196, Thr236, Leu257, Val261, Leu264, Ile268, and Val309. Besides hydrophobic interactions, the carboxylic head group of AA also formed hydrogen bonds with residues Ser321 for AA_1 and Ser306 and Ser325 for AA_2 (Figure 4B). In contrast to Mp1p-LBD2-2AA, the position and also the conformation of AA in Mp1p-LBD2-1AA mostly matched the U-shaped AA_1 and partially overlapped with AA_2 in Mp1p-LBD2-2AA (Figure S5). In consideration of the two-step binding of AA as revealed by NMR and ITC assays, we speculate that the first bound AA would slide backward and fold up to adopt the U-shaped conformation of AA_1 in order to accommodate the second AA (AA_2) on the other side of the cavity (Figure S5). Interactions between the bound AA ligands and the protein were mainly hydrophobic via various non-polar uncharged Ala, Leu, Ile, Val, and Phe residues lying on the surface of the inner cavity (Figure 4B). As such, some hydrophobic interactions between protein residues (Phe196, Thr236, Leu257, Val261, Leu264, Ile268, and Val309) and AA were shared in both one-AA-bound and two-AA-bound states of Mp1p-LBD2. The I332A and V309D mutants were showing quite different titration curves (Figures 2D and 3A) and K_d values for AA binding (Figure 3B) because they each pointed to a different AA ligand binding site. I332 is located at the center of the AA_2 ligand binding site and V309 at the AA_1 ligand binding site (Figure 4B).

AA Was Co-immunoprecipitated with Endogenous Mp1p Protein

To investigate whether endogenous Mp1p could trap AA, co-immunoprecipitation (coIP) assays were performed by using anti-Mp1p monoclonal antibody on *T. marneffei*-infected J774 macrophages (at 30 hr post-infection) and the control non-infected J774 macrophages. AA could be identified in the lipid extract of immunoprecipitated products of the *T. marneffei*-infected cell pellet but not from those of the non-infected cell samples (Figure 5A). Endogenous Mp1p could only be observed by western blotting on the infected cell pellet samples (Figure 5B).

T. marneffei Could Suppress Cellular AA Level and Downstream AA Metabolites and Cytokines Production in Cell Culture

To investigate whether Mp1p can contribute to real reduction of cellular-level AA and the sequential downstream effects after

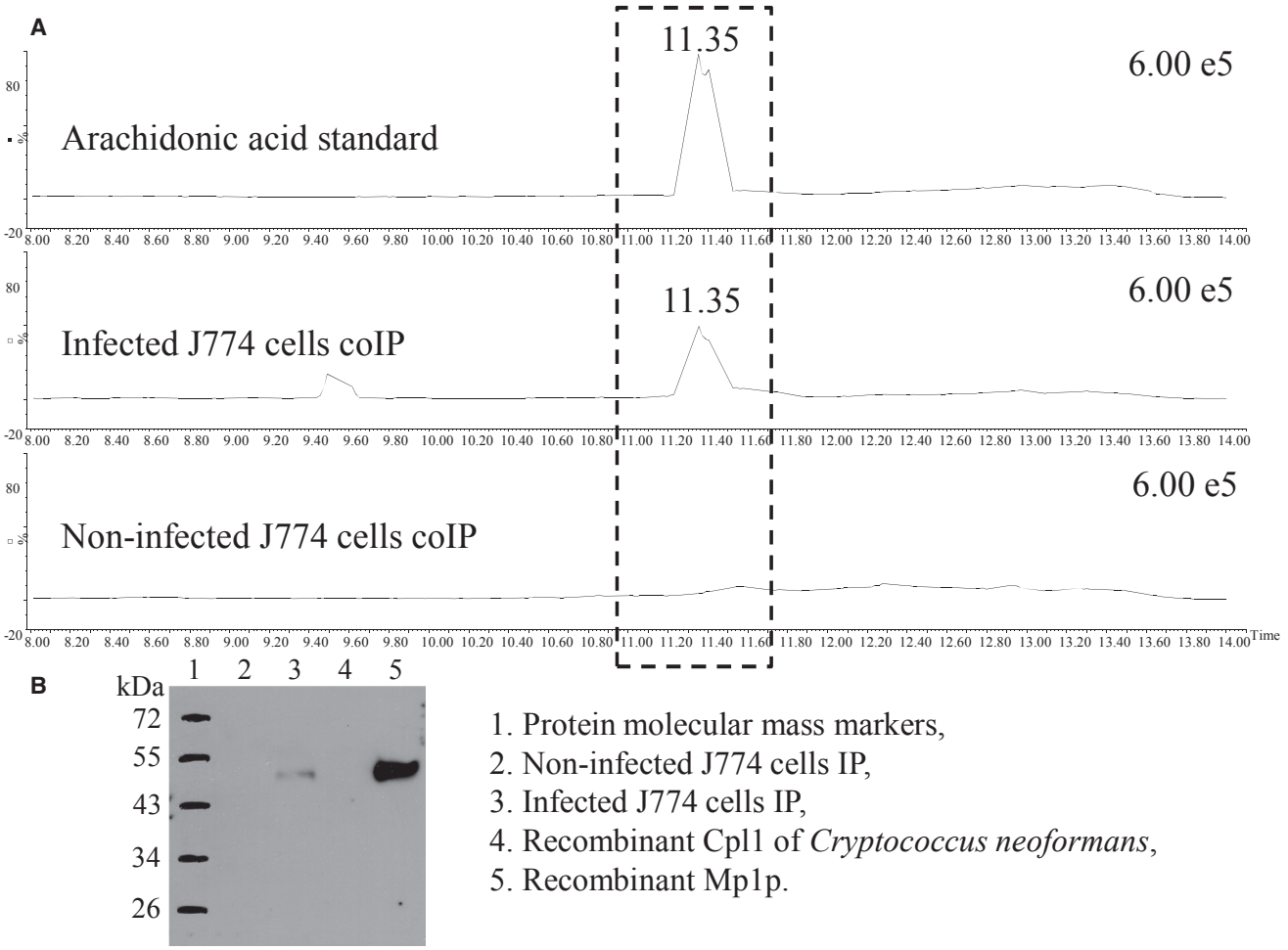

Figure 5. AA Was Co-immunoprecipitated with Endogenous Mp1p Protein

(A) Extracted-ion chromatogram of m/z 303.2/259.2 multiple reaction monitoring (MRM) transition for AA standard (upper trace), for lipid extracts from coIP products of *T. marneffei*-infected J774 cells (middle trace), and for non-infected J774 cells (lower trace).

(B) Western blot showing IP results: lane 1, protein molecular mass markers; lane 2, non-infected J774 cells IP; lane 3, infected J774 cells IP; lane 4, recombinant Cpl1 of *Cryptococcus neoformans*; lane 5, recombinant Mp1p.

T. marneffei infection, we performed a comparative quantitative LC-MS analysis on AA and prostaglandin E2 (PGE2) concentrations in J774 cells infected with wild-type and *MP1* knockout strains of *T. marneffei*. PGE2 is a predominant proinflammatory product of AA metabolism and is synthesized via the COX and prostaglandin synthase pathways (Dennis and Norris, 2015). When a proinflammatory state induced by invading pathogens is sensed, PGE2 is produced and accumulates in the cell culture medium. Figures 6A and 6B show that J774 cells infected with wild-type *T. marneffei* have significantly lower cellular AA concentration at both 7 and 30 hr post-infection compared with those of J774 cells infected with *MP1* knockout strain ($p = 0.00460$ and $p = 0.0317$) or non-infected J774 cells ($p = 0.00130$ and $p = 0.0142$). But the AA concentrations of J774 cells infected with the *MP1* knockout strain *T. marneffei* were not significantly different from those of non-infected J774 cells at both infection time points ($p = 0.0754$ and $p = 0.545$). PGE2 quantification of the cell pellet of J774 cells infected with the *MP1* knockout strain of *T. marneffei* at 7 and 30 hr post-infection showed significantly higher PGE2 levels compared with those of J774 cells infected with wild-type ($p = 0.0255$ and $p = 0.00453$) and non-infected J774 cells ($p = 0.00960$ and $p = 0.000707$) (Figures 6C and 6D). Figures 6E and 6F show that PGE2 levels in the supernatant of J774 cells infected with the *MP1* knockout strain at 7 and 30 hr post-infection were significantly higher compared with those of J774 cells infected with wild-type ($p = 0.000376$ and $p = 0.000374$) and non-infected J774 cells ($p = 0.000626$ and $p = 0.00171$). In contrast, the PGE2 levels in the supernatant of J774 cells infected with wild-type *T. marneffei* at 7 and 30 hr post-infection were significantly lower compared with those of non-infected J774 cells ($p = 0.0205$ and $p = 0.000262$). These results supported the idea that the AA trapping function of Mp1p is associated with reduced levels of cellular AA and subsequently reduced production of PGE2. It should be noted that PGE2 was found to be not interacting with Mp1p-LBD2 by NMR titration experiments (data not shown). Therefore, the reduced production of PGE2 in J774 cells infected with wild-type *T. marneffei* is not due to trapping of PGE2 by Mp1p-LBD2.

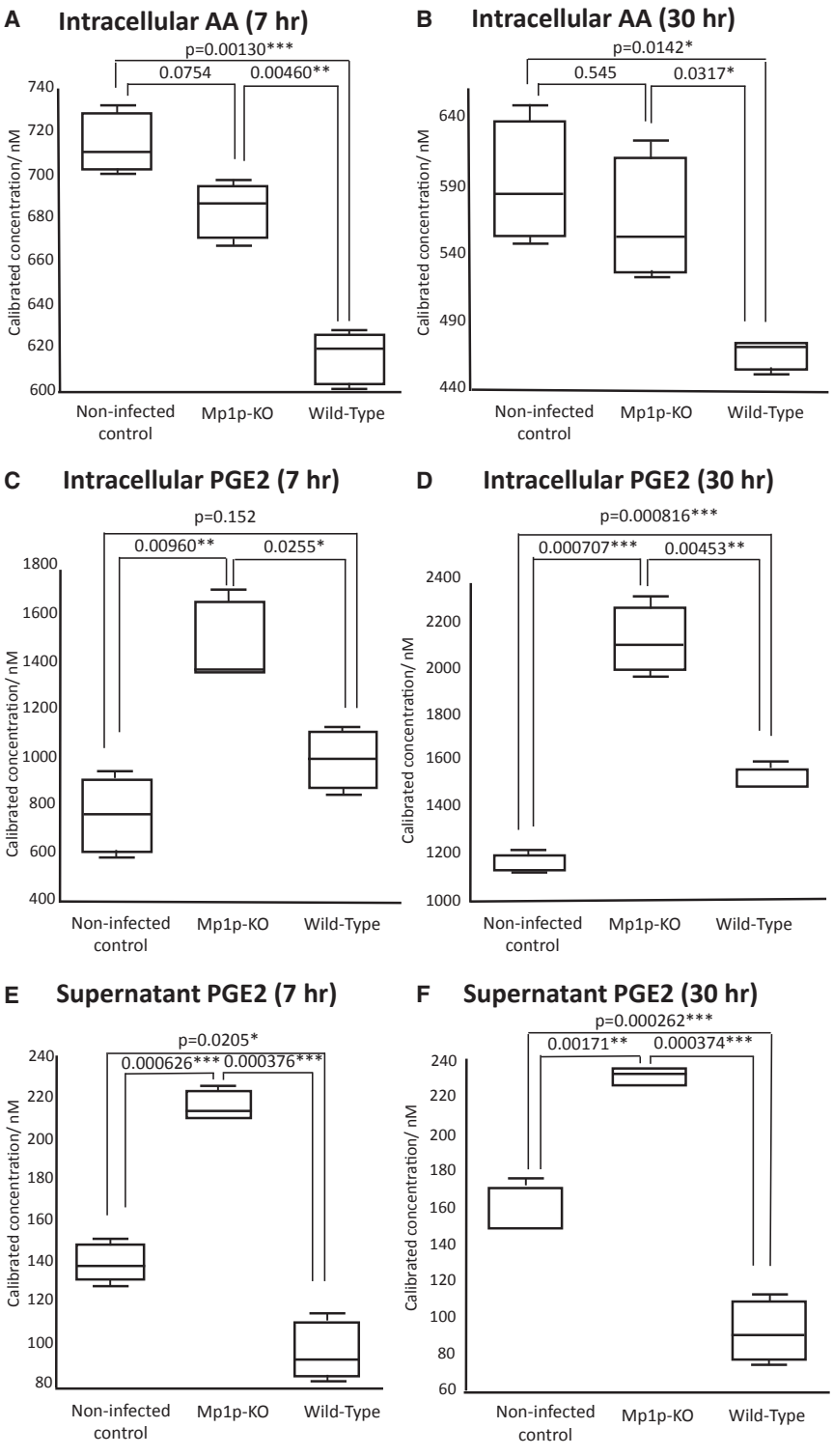

Figure 6. Quantitative LC-MS Analysis on AA and PGE2 Concentrations of J774 Cells Infected with Wild-Type and *MP1* Knockout Strains of *T. marneffei*

The calibrated concentrations of AA and prostaglandin E2 (PGE2) in lipid extracts from intracellular cell lysate and supernatant medium in J774 cells infected with wild-type and *MP1* knockout strains of *T. marneffei* versus non-infected J774 cells as control: intracellular AA concentrations at 7 hr (A) and 30 hr (B) post-infection, intracellular PGE2 concentrations at 7 hr (C) and 30 hr (D) post-infection, and supernatant PGE2 concentrations at 7 hr (E) and 30 hr (F) post-infection. All data are expressed as the mean ± SD in triplicate, and statistically significant differences (p values) among groups were determined by Mann-Whitney U tests (*$p < 0.05$, **$p < 0.01$, ***$p < 0.001$).

We have also measured the relative fold changes of a number of AA metabolites in J774 cells (30 hr post-*T. marneffei* infection) covering the COX, LOX, and CYP450 enzyme pathways (Supplemental Experimental Procedures). There is a general downregulation of these AA metabolites, as shown in Table S4, ranging from −2.14- to −3.27-fold. To evaluate whether the reduction of levels of AA and its metabolites will affect cytokine production, we have performed IL-6 and TNF-α quantification by ELISA for batches of 1×10^6 J774 cells infected with wild-type *T. marneffei*, *MP1* knockout mutant and mock infected (Supplemental Experimental Procedures). Compared with the *MP1* knockout mutant-infected samples, the samples infected with wild-type *T. marneffei* showed lower levels of IL-6 and TNF-α (Figure S6).

Identification of Mp1p-LBD2 Homologs in Other Species

NCBI's conserved domain database (Marchler-Bauer et al., 2015) has placed Mp1p-LBD2 under the hydrophobic surface binding protein A (HsbA) conserved protein domain family. HsbA is found in animal pathogenic and entomopathogenic fungi (Ohtaki et al., 2006), typically 171–275 amino acids in length. A DELTA-BLAST (Domain Enhanced Lookup Time Accelerated BLAST) search (Boratyn et al., 2012) of non-redundant protein sequences database was performed to look for potential Mp1p-LBD2 homologs. The results after filtering the matches for *T. marneffei* are summarized in Table S5. Many putative Mp1p-LBD2 homologs with sequence identity ranging from 10% to 48% could be identified in fungal pathogens, such as *Aspergillus fumigatus* and *Aspergillus flavus*. In our on-going investigations of these Mp1p-LBD2 homologs, we have confirmed that Mp1p-LBD2 homologs Afmp1p, Afmp2p, and Afmp4p of *A. fumigatus* can all bind AA in a similar five-helix bundle fold compared with Mp1p-LBD2. (Full structural and functional characterizations of the binding of AA with Afmp1p, Afmp2p, and Afmp4p will be described in a forthcoming manuscript.) Of

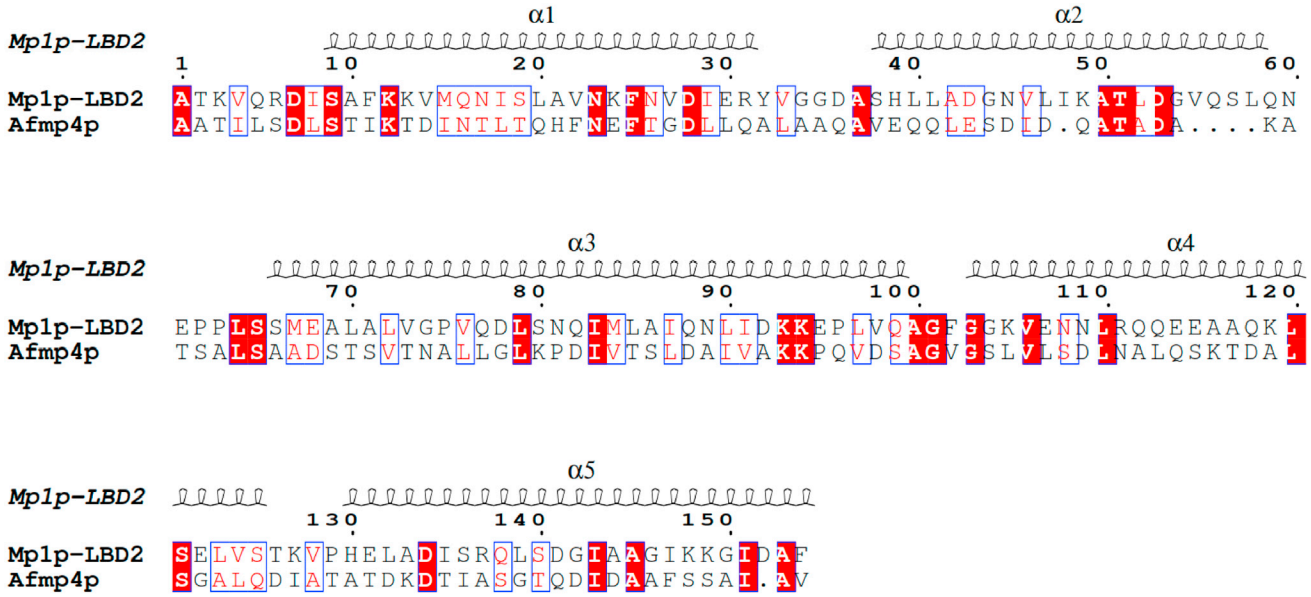

Figure 7. Sequence Alignment of Afmp4p and Mp1p-LBD2
Red shaded letters represent conserved residues. Highly similar residues are colored in red and framed in blue.

particular interest, Afmp4p of *A. fumigatus*, a novel Mp1p-LBD2 homolog having only 18% sequence identity to Mp1p-LBD2 (Figure 7), still forms an almost identical five-helix bundle structure to trap the AA molecule in a central hydrophobic cavity. The titration of AA ligand into apo-Afmp4p induces large chemical shift perturbation changes on many of the amide cross peaks shown in the 2D ^{1}H-^{15}N-HSQC spectra of ^{15}N-labeled Afmp4p protein as well as large raw heats of binding changes (Figure S7), indicative of a strong binding process.

DISCUSSION

In this study, we discovered that AA is the dominant high-affinity cellular target of Mp1p-LBD2 by in vitro pull-down experiments using progressively lower amounts of bait Mp1p-LBD2 proteins. AA is a 20-carbon n-6 polyunsaturated fatty acid (PUFA) and a key proinflammatory signal mediator because it gives rise to the eicosanoid family of mediators. These eicosanoids have potent inflammatory actions even at nanomolar scale. They regulate the production of other mediators including inflammatory cytokines. Since the biosynthesis of eicosanoids depends on the availability of free AA, the concentration of free AA in resting cells is under tight control and kept low by locking excess AA into a phospholipid pool in esterified form by the action of coenzyme A synthetase (Brash, 2001). In response to a variety of cellular stimuli including infection by microbes, phospholipase A2 hydrolyzes the ester bonds in membrane phospholipids to yield lysophospholipids and AA to initiate the inflammatory response. Previous studies have established that diet affects the cell membrane fatty acid (FA) composition of humans and other animals. In rat models, diets that differed in FA profiles produced significant variations in cell membrane FA compositions, with saturated FA content ranging from 8% to 88% of total FAs, monounsaturated FAs (6%–65%), total PUFAs (4%–81%), n-6 PUFAs (3%–70%), and n-3 PUFAs (1%–70%) (Abbott et al., 2012). On average, the membrane phospholipids of cells taken from humans consuming Western-type diets typically contain approximately 20% of total FAs as the n-6 PUFA AA (Calder, 2006). Around 0.5–1 μM free AA on a per volume basis was reported in resting leukocytes (Chilton et al., 1996). In other words, it is expected that the amount of free AA will be substantially lower than other major components in the phospholipid pool such as PC and LPC. Here we have performed quantitation of lipids extracted from the total cell lysis of J774 macrophages. AA was shown to have the lowest cellular level in the list of potential substrates of Mp1p-LBD2, and the total amount of the other lipids found in the list was 67- and 38-fold that of AA under non-infected and LPS-activated states, respectively (Table S2). AA was the only pull-down substrate of Mp1p-LBD2 that could maintain a constant pull-down amount and efficiency from the high to the low bait protein conditions, indicating that Mp1p-LBD2 possessed a higher affinity for AA than other more abundant competing lipids. Since AA was the dominant lipid pulled down at the lowest bait protein condition (Figure 1A), AA is expected to be the dominant cellular target of Mp1p-LBD2 protein during the early stage of *T. marneffei* infection when the cellular Mp1p concentration is low. This is further supported by the co-immunoprecipitation of AA with endogenous Mp1p protein shown in Figure 5.

We have validated and characterized the tight binding of AA with Mp1p-LBD2 by NMR titration experiment, ITC measurement, and X-ray crystallography. The structures of Mp1p-LBD2 complexed with one or two AAs presented here both showed a closed monomeric five-helix bundle fold, with total length about 47 Å (Figure 4). This five-helix bundle fold of Mp1p-LBD2 for AA encapsulation is unique among the structures of other known AA-binding proteins. To date, known common intracellular AA-binding proteins include most FA-binding proteins (FABPs) (see Smathers and Petersen, 2011 for review) and the enzymes catalyzing the

first step of conversion from released AA to various downstream eicosanoids (COXs and LOXs). FABPs possess a highly conserved mobile N-terminal helix-turn-helix motif to encapsulate hydrophobic ligands reversibly in their hydrophobic cavities, including AA. It is thought that the presence of mobile "lid-like" structures is important for efficient loading and unloading of hydrophobic ligands carried by FABPs. Channels to internal active sites of COXs and LOXs are always observed on protein surfaces to allow exchange of AA substrate and the products. The highly enclosed hydrophobic cavity of Mp1p-LBD2 is thus unusual and may contribute to the significantly smaller K_d value of the first AA binding (13 nM by ITC) compared with the smallest reported value of 179 nM in FABP2 by ITC (Baier et al., 1995). This relatively higher affinity binding of AA by Mp1p-LBD2 is expected to be critical for the proposed biological function of Mp1p-LBD2, as this will allow AA to be more readily captured by Mp1p-LBD2 than by other AA-binding proteins in the host.

The unusual ability to trap two molecules of AA by Mp1p-LBD2, as indicated by the titration experiments using NMR and ITC methods (Figures 2 and 3), was confirmed by X-ray crystallography (Figure 4B). The majority of the interactions between Mp1p-LBD2 and the bound ligand were hydrophobic interactions and a few hydrogen bond interactions toward the polar carboxylic head groups of the AA ligands (Figure 4B). Therefore, some subsequent single point mutations (I332A and V309D) can significantly weaken and reduce the binding of AA to a one-state binding (Figures 2D and 3A). It is conceivable that Mp1p-LBD2 is designed to trap more than one AA molecule to increase its trapping efficiency in cells. As far as we know, all known AA-binding FABPs, COXs, and LOXs interact with one molecule of AA per binding site. Physiologically, this ability to trap more than one AA molecule per Mp1p-LBD2 will improve the efficiency of anti-inflammatory action by Mp1p through encapsulation of AA, which will be critical at the initial stage of the *T. marneffei* infection. Furthermore, the plasticity of Mp1p-LBD2 to bind one or two AA molecules with different affinities may reflect the flexibility of this class of AA-binding proteins to sequester AA in response to the abundance of available inflammatory mediators generated by the host, and presents a novel way of manipulating the host response at the level of protein-ligand interactions. To our knowledge, this is the first time that a virulence factor from a microbial pathogen has been shown by crystal structures to have the plasticity to bind one or more than one target inflammatory mediators.

The in vivo trapping of AA by Mp1p was confirmed by our co-immunoprecipitation experiment (Figure 5). But further experiments were needed to demonstrate the biological impacts of AA capturing by Mp1p. Quantitative LC-MS lipid analysis showed that J774 cells infected with wild-type *T. marneffei* have significantly lower levels of cellular AA compared with non-infected J774 cells, indicating that the continuous secretion of Mp1p by *T. marneffei* caused a reduction of cellular AA level. In parallel, we have also observed downstream AA metabolite reductions under each of the COX, LOX, and CYP450 pathways (Table S4). However, no significant changes of AA levels were observed for J774 cells infected with the *MP1* knockout strain of *T. marneffei* (Figures 6A and 6B) as no Mp1p was expected to be expressed by the *MP1* knockout strain. Moreover, we also observed significantly increased production of IL-6 and TNF-α for the *MP1* knockout strain-infected J774 cells (Figure S6). These results strongly support the idea that the observed trapping of AA by Mp1p-LBD2 does have biological consequences of lowering the cellular AA level and the subsequent suppression of the downstream AA metabolites and proinflammatory cytokines IL-6 and TNF-α. To our knowledge this is the first report of a virulence factor targeting the proinflammatory AA molecule to reduce the inflammatory response.

Our NCBI DELTA-BLAST search performed with the Mp1p-LBD2 sequence indicated that Mp1p-LBD2 homologous proteins could be found in many pathogenic fungi with sequence identity ranging from 10% to 48% (Table S5). In our previous studies, we have cloned and characterized a number of secretory cell wall mannoprotein homologs of Mp1p of *T. marneffei* for serodiagnosis, including Afmp1p and Afmp2p of *A. fumigatus* and Aflmp1p of *A. flavus* (Chan et al., 2002; Chong et al., 2004; Wang et al., 2012; Woo et al., 2002, 2006, 2003; Yuen et al., 2001). *A. fumigatus* and *A. flavus* are the most prominent opportunistic fungal pathogens in immunocompromised hosts, causing aspergilloma and invasive aspergillosis globally. Our on-going investigation indicated that Afmp1p, Afmp2p, and Afmp4p of *A. fumigatus* were also AA-binding proteins capable of trapping AA molecules in a fashion similar to that of Mp1p-LBD2. Of interest, the novel Afmp4p protein of *A. fumigatus*, with only 18% sequence identity to Mp1p-LBD2, not only has a similar structure to that of Mp1p-LBD2 but also similar strong binding properties toward AA (Figure S7). Therefore, this novel mechanism of host innate immunity evasion of *T. marneffei* through the trapping of a key proinflammatory signaling lipid may be conserved in other fungal pathogens. Mp1p-LBD2 thus represents a novel class of FABPs with the function of targeting a key proinflammatory signaling lipid to dampen the host innate immune response. We are now in the process of characterizing other Mp1p-LBD2 homologs identified in the present study. Most human pathogenic fungi affecting the lung are mold or dimorphic fungi such as *A. fumigatus* or *T. marneffei*. They produce spores or conidia, which are spread in the air with counts often exceeding billions per cubic meter. Once they arrive at the alveoli of our lungs, they are ingested by our tissue macrophages. A previous study showed that the surface hydrophobic RodA protein on the surface of the dormant *A. fumigatus* conidia masks their recognition by the host innate immune cells such as macrophage or dendritic cells (Aimanianda et al., 2009). However, these conidia or spores must germinate into fungal hyphae or yeast form in order to cause a progressive infection in the host. How these germinating conidia, hyphae, or yeast forms evade the proinflammatory innate immune response remains elusive. Here, we showed that these fungi may produce Mp1p or its homologs, which could capture AA to stall the inflammatory process.

SIGNIFICANCE

T. marneffei is the most important thermally dimorphic fungus causing systemic mycosis in HIV-positive patients in China and Southeast Asia. We recently showed, in a related work, that the secreted protein Mp1p is a novel virulence factor of _T. marneffei_ in a mouse model. Yet the mechanism governing its virulence was unknown. By pull-down experiments, we showed that Mp1p-LBD2 has high affinity for a

key human proinflammatory lipid mediator, arachidonic acid (AA). We further characterized this interaction in detail and found that AA-bound Mp1p-LBD2 is a monomer, which is different from the previously reported dimeric structure between Mp1p-LBD2 and palmitic acid. Our structure revealed that Mp1p-LBD2 formed a five-helix bundle fold to create a long hydrophobic central cavity for high-affinity encapsulation of AA. Mp1p-LBD2 also has an unusual plasticity of binding one or two AA molecules depending on the availability of AA to enhance its trapping efficiency. Finally, we showed in cell-based analysis that the AA-capturing property of Mp1p is functionally relevant because *T. marneffei* is able to reduce the availability of cellular AA and decrease the production of downstream AA metabolites, IL-6 and TNF-α. Therefore, this work has contributed toward a better understanding of the function of a novel class of virulence factor, Mp1p in *T. marneffei*, and provided important insight into the host defense evasion and pathogenesis by *T. marneffei*. Given that homologous proteins with structure and function similar to those of Mp1p-LBD2 have been identified in other fungal pathogen such as *A. fumigatus*, this novel mechanism of host innate immune evasion through capturing of a proinflammatory signaling lipid may have a broad implication for fungal pathogenesis. The knowledge obtained in this work may lead to the development of better chemotherapeutic intervention in fungal diseases in the future.

EXPERIMENTAL PROCEDURES

Strain of *T. marneffei* and Cell Cultures of J774 Macrophages

All fungal strains were grown on Sabouraud dextrose agar at 25°C or 37°C. *T. marneffei* strain *PM1* was isolated from an HIV-negative patient suffering from culture-documented penicilliosis in Hong Kong. The *MP1* knockout strain was generated as previously described (Woo et al., 2016). The murine macrophage-like J774 cell line was obtained from ATCC (ATCC No. TIB-67).

Cloning, Overexpression, and Purification of Mp1p-LBD2

To produce a fusion plasmid for protein purification, primers were used to amplify the *MP1* gene (Genbank: KFX52825.1) from the *MP1* plasmid described previously (Cao et al., 1998). The sequence coding for amino acid 187 to 346 of Mp1p-LBD2 was sub-cloned into a pET-22b (+) vector using standard cloning protocols. The resulting His-tagged protein was transformed and expressed in *E. coli* strain BL21 (DE3) and purified with a HiTrap nickel-chelating affinity column (GE Healthcare) according to the manufacturer's protocols. The protein was further purified by size-exclusion chromatography on a Superdex HiLoad 16/60 S75 prep-grade column (GE Healthcare). To obtain ^{15}N- or $^{15}N/^{13}C$-labeled protein samples for the NMR studies, expression was performed in M9 medium with 1.0 g/L $^{15}NH_4Cl$ or together with 2.0 g/L [^{13}C]glucose (Cambridge Isotopes Laboratory) after 0.1 mM isopropyl-β-D-1-thiogalactopyranoside (IPTG) induction at 37°C as previously described (Tse et al., 2011). To ensure that the purified protein had no pre-trapped lipid ligand bound inside its hydrophobic cavity, extensive delipidation was carried out on the Mp1p-LBD2 protein samples. Briefly, each sample was delipidated by extracting the protein solution three times with an equal volume of diisopropyl ether:n-butanol (3:2) for 30 min with gentle shaking. The protein solution was then dialyzed against a buffer (20 mM Tris [pH 8.0]) to remove n-butanol before pull-down experiments, ITC, and NMR measurements.

Pull-Down Experiment on the Cell Lysate of J774 Macrophage Cells with Mp1p-LBD2

The J774 murine macrophage cell line was grown in DMEM (Invitrogen) supplemented with 10% heat-inactivated fetal bovine serum (FBS) at 37°C. LPS-induced inflammatory response was achieved by stimulating the macrophage with 1 μg/mL LPS at 37°C for 24 hr. The cells were harvested from confluent cultures and washed three times with 1× PBS buffer at 4°C. Cell suspensions in 1× PBS containing 3 × 10^6 cells per tube were mixed with 1,000, 250, or 50 μg of soluble delipidated His-tagged Mp1p-LBD2 protein on ice. The mixture was immediately sonicated on ice for 20 s, followed by incubation on ice for 30 min in the presence of 10 μg/mL Complete protease inhibitor mixture (Roche Applied Science). After centrifugation at 10,000 × *g* for 15 min, the supernatant was removed and incubated with 30 μL of Ni-NTA agarose resin (QIAGEN) at 4°C for 30 min. The resin was washed with 20 column volumes of 1× PBS buffer supplemented with 10 mM imidazole. Lipid-bound Mp1p-LBD2 protein was eluted with 200 μL of PBS buffer containing 200 mM imidazole. Lipid in the Mp1p-LBD2 protein was extracted by incubating with organic solvent (diisopropyl ether and n-butanol mixture [3:2 v/v]) at 1:1 ratio for 30 min at room temperature. The organic layer was separated by centrifugation (2 min, 13,000 rpm) and subjected to untargeted small-molecule profiling by ultra-high-performance liquid chromatography-electrospray ionization-quadruple time-of-flight mass spectrometry (UHPLC-ESI-QTOFMS) using the lipid profiling method to analyze lipid species as we have previously described (To et al., 2015, 2016). Control pull-down experiments were performed under the same procedures except no Mp1p-LBD2 protein was added to the J774 cells. Three biological replicates were performed for each pull-down experiment, and triplicate measurements were made for each pull-down condition. Detailed MS data acquisition methodology and analysis of the pull-down extraction samples are presented in the Supplemental Experimental Procedures.

Co-immunoprecipitation of Endogenous Mp1p Protein

Cell suspensions containing 2 × 10^6 *T. marneffei*-infected (at 30 hr post-infection) and control non-infected J774 macrophages were prepared as described for the pull-down experiment. Cells were lysed by brief sonication in PBS buffer. Lysates were centrifuged for 10 min at 24,000 × *g*. The clear supernatant was incubated at 4°C for 120 min with anti-Mp1p monoclonal antibodies prepared as we previously described (Wang et al., 2011). Thirty microliters of pre-washed protein G agarose beads (IP50, Sigma-Aldrich) was added and incubated for another 120 min at 4°C. The immunoprecipitation (IP) product was collected by centrifugation for 10 min at 24,000 × *g*. After extensive washing, the IP product was subjected to lipid extraction and LC-MS analysis as described in the Supplemental Experimental Procedures. Triplicate measurements were made for each experimental condition. A solvent control was included in the LC-MS analysis.

Comparative Quantitative LC-MS Analysis of Lipid Extracts from Cell Lysate of J774 Cells Infected with Wild-Type and *MP1* Knockout Strains of *T. marneffei*

The J774 murine macrophage cell line was grown in DMEM (Invitrogen) supplemented with 10% heat-inactivated FBS at 37°C. Yeast cells of wild-type *T. marneffei* or the *MP1* knockout strain of *T. marneffei* were added to J774 macrophages at an MOI of 10 and incubated at 37°C with 5% CO_2. After 2 hr, macrophage monolayers were washed sequentially with 240 U/mL nystatin (Sigma) and warm Hank's buffered salt solution to kill extracellular fungi. At each designated time point of infection (7 and 30 hr), triplicate 3 × 10^6 macrophage samples were first harvested from confluent cultures and washed three times with 1× PBS buffer at 4°C and then 5 mL of the supernatant samples was filtered and collected. Both cell pellet and supernatant samples were freeze-dried and resuspended in 60% methanol in water followed by subsequent pulse sonication at 4°C with a probe sonicator (Vibra Cell; Sonics & Madell Technology) for ten rounds of 30 s sonication (50% duty cycle, 20% amplitude). The organic layer was separated by centrifugation (2 min, 13,000 rpm) and subjected to targeted small-molecule quantitative analysis of AA, PGE2, and other pro- and anti-inflammatory lipid mediators produced from AA (PGD2, HETE, leukotriene A4, leukotriene B4, etc.) by ultra-high-performance liquid chromatography-electrospray ionization-QTRAP mass spectrometry (UHPLC-ESI-QTRAP-MS/MS) (Supplemental Experimental Procedures). The UHPLC-ESI-QTRAP-MS/MS analysis was carried out using an AB SCIEX 6500QTRAP tandem MS system. Triplicate non-infected J774 macrophage samples of 3 × 10^6 cells were also collected as

controls and subjected to the same sample preparation and analysis protocol as described above.

NMR Chemical Shift Perturbation Titration

Two-dimensional ^{1}H-^{15}N HSQC NMR spectra of delipidated ^{15}N-labeled Mp1p-LBD2 (300 μM) in 20 mM sodium phosphate buffer (pH 6.8), 100 mM NaCl, 90% H_2O/10% D_2O were monitored upon addition of increasing amounts of AA (20 mM stock solution). A series of 2D ^{1}H-^{15}N HSQC spectra was recorded at 298 K at AA:Mp1p-LBD2 molar ratios of 0:1, 0.25:1, 0.5:1, 0.75:1, 1:1, 1.25:1, 1.5:1, 1.75:1, 2:1, 2.5:1, and 3:1. The titration experiment was performed in duplicate. All experiments were performed on a Bruker Avance 600 MHz NMR spectrometer (Bruker) as described previously (Tse et al., 2012). The NMR spectra were acquired and processed by the software Topspin 3.1 (Bruker) and analyzed by NMRFAM-SPARKY (Lee et al., 2015).

Affinity Measurements of Mp1p-LBD2 Binding with AA by Isothermal Titration Calorimetry

Delipidated wild-type or mutated Mp1p-LBD2 protein samples (100 μM) were loaded into the sample cells and titrated with an AA stock solution of 10 mM by an iTC_{200} microcalorimeter (Ultrasensitive Calorimetry for the Life Science, MicroCal). The starting temperature was 37°C, and the reference in the reference cell was pure autoclaved water. The titrations were performed by injecting 20 consecutive 5 μL aliquots of AA stock solution into the ITC cell containing the Mp1p-LBD2 sample. The titration experiment was performed in triplicate. The binding stoichiometry (n), binding affinity (K_A), enthalpy changes (ΔH), and entropy (ΔS) of the protein-ligand interaction were determined by analyzing the resulting ITC data with the software ORIGIN 7 using appropriate binding models.

Crystal Structure Determination of Mp1p-LBD2 with AA

Recombinant Mp1p-LBD2 expressed in *E. coli* was delipidated first and mixed with an equal molar ratio of AA before crystallization. Crystals of Mp1p-LBD2-1AA were obtained using the hanging-drop vapor-diffusion method by mixing 1 μL of protein-ligand complex (30 mg/mL) with 1 μL of reservoir buffer (0.2 M ammonium acetate, 0.1 M sodium acetate [pH 4.8], and 26% [w/v] PEG4000) at 298 K. The crystals were soaked in cryo-protectant (0.2 M ammonium acetate, 0.1 M sodium acetate [pH 4.8], 26% [w/v] PEG4000, and 16% glycerol) and flash-frozen into liquid nitrogen. Datasets of Mp1p-LBD2-1AA were collected at wavelength of 0.9793 Å and temperature of 100 K at beamline BL17U in the Shanghai Synchrotron Radiation Facility. Data reduction was performed with the HKL2000 (Minor, 1997) program suite. Mp1p-LBD2-1AA was solved by the molecular replacement method using Phaser (McCoy et al., 2007) in the CCP4 package (Collaborative Computational Project Network, 1994) and the apo-Mp1p-LBD2 structure (PDB: 3L1N) was used as the search model. There were four Mp1p-LBD2 molecules in one asymmetric unit. Model building and refinement were performed with cycles of manual adjustment using Coot (Emsley and Cowtan, 2004) and Refmac5 (Murshudov et al., 1997) in the CCP4 package. Crystals of Mp1p-LBD2 complexed with two AAs were obtained with the same crystallization conditions and method as Mp1p-LBD2-1AA crystals but with 3-fold molar excess of AA added before crystallization. Datasets of Mp1p-LBD2-2AA at resolution of 1.50 Å were collected at wavelength of 0.9793 Å and temperature of 100 K. Data analysis and structure refinement procedures were the same as for Mp1p-LBD2-1AA except molecular replacement was performed with Mp1p-LBD2-1AA solved in this study as the search model. There were four Mp1p-LBD2 molecules in an asymmetric unit. Data collection and structure refinement statistics are listed in Table S6. Both structures were analyzed with MolProbity (Davis et al., 2007) showing that all the residues of both structures were in the favored regions of a Ramachandran plot. All the graphical presentations of the structures were prepared with PyMOL (http://www.pymol.org/).

ACCESSION NUMBERS

Coordinates and structure factors for Mp1p-LBD2-1AA and Mp1p-LBD2-2AA have been deposited in PDB with accession codes PDB: 5CSD and 5FB7, respectively.

SUPPLEMENTAL INFORMATION

Supplemental Information includes Supplemental Experimental Procedures, seven figures, and six tables and can be found with this article online at http://dx.doi.org/10.1016/j.chembiol.2016.12.014.

AUTHOR CONTRIBUTIONS

K.Y.Y., Q.H., R.Y.T.K., and K.H.S. planned and organized the experiments. W.H.L., Y.H.K., and M.K.T. performed protein expression and purification. W.H.L. and H.M.Z. performed crystallization, diffraction experiments, and structure determination. M.K.T. performed the J774 cell cultures and lipid pull-down experiments. K.H.S. and R.K.C.L. performed the NMR titration experiments. S.X. performed the ITC experiment. P.C.Y.W., S.K.P.L., E.T.K.T., and C.C.Y.L. generated stable J774 cell lines and the wild-type and knockout strains of *T. marneffei*. J.P.C. and Y.H.K. performed the coIP experiments. Y.H.K. performed the LC-MS/MS experiments. K.H.S., W.H.L., Y.H.K., R.Y.T.K., M.K.T., and K.Y.Y. wrote the manuscript.

ACKNOWLEDGMENTS

We thank Dr. Stanley Kwok-Kuen Cheung and Dr. Kim-Chung Lee for helpful suggestions on the pull-down and LC-MS experiments, respectively. This work was supported by a donation from Mr. Michael Tong and the Providence Foundation in memory of Mr. and Mrs. L.H.M. Lui; the Health and Medical Research Fund (commissioned study) of the Food and Health Bureau of Hong Kong Special Administrative Region (HKM-15-M05, HKM-15-M07); the Research Grant Council Fund of Hong Kong (GRF777512); Natural Science Foundation of China grants (31370739 and 31670753); and research grants from the Shenzhen government (ZDSYS20140509142721429) and from SUSTC (FRG-SUSTC1501A-24). We thank the Shanghai Synchrotron Radiation Facility for technical support.

Received: April 19, 2016
Revised: October 19, 2016
Accepted: December 21, 2016
Published: January 19, 2017

REFERENCES

Abbott, S.K., Else, P.L., Atkins, T.A., and Hulbert, A.J. (2012). Fatty acid composition of membrane bilayers: importance of diet polyunsaturated fat balance. Biochim. Biophys. Acta *1818*, 1309–1317.

Aimanianda, V., Bayry, J., Bozza, S., Kniemeyer, O., Perruccio, K., Elluru, S.R., Clavaud, C., Paris, S., Brakhage, A.A., Kaveri, S.V., et al. (2009). Surface hydrophobin prevents immune recognition of airborne fungal spores. Nature *460*, 1117–U1179.

Baier, L.J., Sacchettini, J.C., Knowler, W.C., Eads, J., Paolisso, G., Tataranni, P.A., Mochizuki, H., Bennett, P.H., Bogardus, C., and Prochazka, M. (1995). An amino acid substitution in the human intestinal fatty acid binding protein is associated with increased fatty acid binding, increased fat oxidation, and insulin resistance. J. Clin. Invest. *95*, 1281–1287.

Boratyn, G.M., Schaeffer, A.A., Agarwala, R., Altschul, S.F., Lipman, D.J., and Madden, T.L. (2012). Domain enhanced lookup time accelerated BLAST. Biol. Direct *7*, 12.

Brash, A.R. (2001). Arachidonic acid as a bioactive molecule. J. Clin. Invest. *107*, 1339–1345.

Calder, P.C. (2006). Polyunsaturated fatty acids and inflammation. Prostaglandins Leukot. Essent. Fatty Acids *75*, 197–202.

Cao, L., Chan, C.M., Lee, C., Wong, S.S., and Yuen, K.Y. (1998). MP1 encodes an abundant and highly antigenic cell wall mannoprotein in the pathogenic fungus Penicillium marneffei. Infect. Immun. *66*, 966–973.

Cao, L., Chan, K.M., Chen, D., Vanittanakom, N., Lee, C., Chan, C.M., Sirisanthana, T., Tsang, D.N., and Yuen, K.Y. (1999). Detection of cell wall mannoprotein Mp1p in culture supernatants of Penicillium marneffei and in sera of penicilliosis patients. J. Clin. Microbiol. *37*, 981–986.

Chan, C.M., Woo, P.C.Y., Leung, A.S.P., Lau, S.K.P., Che, X.Y., Cao, L., and Yuen, K.Y. (2002). Detection of antibodies specific to an antigenic cell wall galactomannoprotein for serodiagnosis of *Aspergillus fumigatus* aspergillosis. J. Clin. Microbiol. *40*, 2041–2045.

Chilton, F.H., Fonteh, A.N., Surette, M.E., Triggiani, M., and Winkler, J.D. (1996). Control of arachidonate levels within inflammatory cells. Biochim. Biophys. Acta *1299*, 1–15.

Chong, K.T.K., Woo, P.C.Y., Lau, S.K.P., Huang, Y., and Yuen, K.Y. (2004). AFMP2 encodes a novel immunogenic protein of the antigenic mannoprotein superfamily in *Aspergillus fumigatus*. J. Clin. Microbiol. *42*, 2287–2291.

Collaborative Computational Project Network (1994). The CCP4 suite: programs for protein crystallography. Acta Crystallogr. D Biol. Crystallogr. *50*, 760–763.

Cooper, C.R., and Vanittanakom, N. (2008). Insights into the pathogenicity of *Penicillium marneffei*. Future Microbiol. *3*, 43–55.

d'Enfert, C. (2009). Hidden killers: persistence of opportunistic fungal pathogens in the human host. Curr. Opin. Microbiol. *12*, 358–364.

Davis, I.W., Leaver-Fay, A., Chen, V.B., Block, J.N., Kapral, G.J., Wang, X., Murray, L.W., Arendall, W.B., 3rd, Snoeyink, J., Richardson, J.S., et al. (2007). MolProbity: all-atom contacts and structure validation for proteins and nucleic acids. Nucleic Acids Res. *35*, W375–W383.

Dennis, E.A., and Norris, P.C. (2015). Eicosanoid storm in infection and inflammation. Nat. Rev. Immunol. *15*, 511–523.

Emsley, P., and Cowtan, K. (2004). Coot: model-building tools for molecular graphics. Acta Crystallogr. D Biol. Crystallogr. *60*, 2126–2132.

Lee, W., Tonelli, M., and Markley, J.L. (2015). NMRFAM-SPARKY: enhanced software for biomolecular NMR spectroscopy. Bioinformatics *31*, 1325–1327.

Liao, S., Tung, E.T., Zheng, W., Chong, K., Xu, Y., Dai, P., Guo, Y., Bartlam, M., Yuen, K.Y., and Rao, Z. (2010). Crystal structure of the Mp1p ligand binding domain 2 reveals its function as a fatty acid-binding protein. J. Biol. Chem. *285*, 9211–9220.

Marchler-Bauer, A., Derbyshire, M.K., Gonzales, N.R., Lu, S., Chitsaz, F., Geer, L.Y., Geer, R.C., He, J., Gwadz, M., Hurwitz, D.I., et al. (2015). CDD: NCBI's conserved domain database. Nucleic Acids Res. *43*, D222–D226.

McCoy, A.J., Grosse-Kunstleve, R.W., Adams, P.D., Winn, M.D., Storoni, L.C., and Read, R.J. (2007). Phaser crystallographic software. J. Appl. Crystallogr. *40*, 658–674.

Minor, Z.O.W. (1997). Processing of X-ray diffraction data collected in oscillation mode. Methods Enzymol. *276*, 307–326.

Murshudov, G.N., Vagin, A.A., and Dodson, E.J. (1997). Refinement of macromolecular structures by the maximum-likelihood method. Acta Crystallogr. D Biol. Crystallogr. *53*, 240–255.

Ohtaki, S., Maeda, H., Takahashi, T., Yamagata, Y., Hasegawa, F., Gomi, K., Nakajima, T., and Abe, K. (2006). Novel hydrophobic surface binding protein, HsbA, produced by *Aspergillus oryzae*. Appl. Environ. Microbiol. *72*, 2407–2413.

Smathers, R.L., and Petersen, D.R. (2011). The human fatty acid-binding protein family: evolutionary divergences and functions. Hum. Genomics *5*, 170–191.

To, K.K.W., Lee, K.C., Wong, S.S.Y., Lo, K.C., Lui, Y.M., Jahan, A.S., Wu, A.L., Ke, Y.H., Law, C.Y., Sze, K.H., et al. (2015). Lipid mediators of inflammation as novel plasma biomarkers to identify patients with bacteremia. J. Infect. *70*, 433–444.

To, K.K., Lee, K.-C., Wong, S.S., Sze, K.-H., Ke, Y.-H., Lui, Y.-M., Tang, B.S., Li, I.W., Lau, S.K., and Hung, I.F. (2016). Lipid metabolites as potential diagnostic and prognostic biomarkers for acute community acquired pneumonia. Diagn. Microbiol. Infect. Dis. *85*, 249–254.

Tse, M.K., Hui, S.K., Yang, Y.H., Yin, S.T., Hu, H.Y., Zou, B., Wong, B.C.Y., and Sze, K.H. (2011). Structural analysis of the UBA domain of X-linked inhibitor of apoptosis protein reveals different surfaces for ubiquitin-binding and self-association. PLoS One *6*, e28511.

Tse, M.K., Cho, C.K., Wong, W.F., Zou, B., Hui, S.K., Wong, B.C.Y., and Sze, K.H. (2012). Domain organization of XAF1 and the identification and characterization of XIAPRING-binding domain of XAF1. Protein Sci. *21*, 1418–1428.

Ustianowski, A.P., Sieu, T.P., and Day, J.N. (2008). *Penicillium marneffei* infection in HIV. Curr. Opin. Infect. Dis. *21*, 31–36.

Vanittanakom, N., Cooper, C.R., Jr., Fisher, M.C., and Sirisanthana, T. (2006). *Penicillium marneffei* infection and recent advances in the epidemiology and molecular biology aspects. Clin. Microbiol. Rev. *19*, 95–110.

Wang, Y.F., Cai, J.P., Wang, Y.D., Dong, H., Hao, W., Jiang, L.X., Long, J., Chan, C., Woo, P.C., Lau, S.K., et al. (2011). Immunoassays based on *Penicillium marneffei* Mp1p derived from *Pichia pastoris* expression system for diagnosis of penicilliosis. PLoS One *6*, e28796.

Wang, Z.Y., Cai, J.P., Qiu, L.W., Hao, W., Pan, Y.X., Tung, E.T.K., Lau, C.C.Y., Woo, P.C.Y., Lau, S.K.P., Yuen, K.Y., et al. (2012). Development of monoclonal antibody-based galactomannoprotein antigen-capture ELISAs to detect *Aspergillus fumigatus* infection in the invasive aspergillosis rabbit models. Eur. J. Clin. Microbiol. Infect. Dis. *31*, 2943–2950.

Wong, S.S.Y., Siau, H., and Yuen, K.Y. (1999). *Penicilliosis marneffei* - West meets East. J. Med. Microbiol. *48*, 973–975.

Woo, P.C.Y., Chan, C.M., Leung, A.S.P., Lau, S.K.P., Che, X.Y., Wong, S.S.Y., Cao, L., and Yuen, K.Y. (2002). Detection of cell wall galactomannoprotein Afmp1p in culture supernatants of *Aspergillus fumigatus* and in sera of aspergillosis patients. J. Clin. Microbiol. *40*, 4382–4387.

Woo, P.C.Y., Chong, K.T.K., Lau, C.C.Y., Wong, S.S.Y., Lau, S.K.P., and Yuen, K.Y. (2006). A novel approach for screening immunogenic proteins in *Penicillium marneffei* using the Delta AFMP1 Delta AFMP2 deletion mutant of *Aspergillus fumigatus*. FEMS Microbiol. Lett. *262*, 138–147.

Woo, P.C.Y., Chong, K.T.K., Leung, A.S.P., Wong, S.S.Y., Lau, S.K.P., and Yuen, K.Y. (2003). AFLMP1 encodes an antigenic cell wall protein in *Aspergillus flavus*. J. Clin. Microbiol. *41*, 845–850.

Woo, P.C.Y., Lau, S.K.P., Lau, C.C.Y., Tung, E.T.K., Chong, K.T.K., Yang, F.J., Zhang, H.M., Lo, R.K.C., Cai, J.P., Au-Yeung, R.K.H., et al. (2016). Mp1p is a virulence factor in *Talaromyces* (Penicillium) *marneffei*. PLoS Negl. Trop. Dis. *10*, e0004907.

Yuen, K.Y., Chan, C.M., Chan, K.M., Woo, P.C.Y., Che, X.Y., Leung, A.S.P., and Cao, L. (2001). Characterization of AFMP1: a novel target for serodiagnosis of aspergillosis. J. Clin. Microbiol. *39*, 3830–3837.